PARTICLE IDENTIFICATION IN COMPASS RICH 1

Progress Report - May 2000.

P. Schiavon

1 INTRODUCTION

This report is an update of the PID section of the Progress Report [1], to which I will refer for all the details.
In [1] the mass assignment to particles for which a *ring* has been reconstructed is done on a χ^2 basis; in the present report, a Likelihood analysis is introduced and the results discussed.

2 PARTICLE IDENTIFICATION ON χ^2 BASIS

a) First approach.

Let here recall some details of the approach already presented in [1].
For a given mass hypothesis and from the (measured) particle momentum, the particle β is calculated and checked for being over the Cherenkov emission threshold; in this case, θ^{ring}_{mass} is calculated as $\cos\theta^{ring}_{mass} = (\beta n)^{-1}$, with n the radiator refraction index (without any correction, at present).
A χ^2_{mass} is then computed summing over N^{photon}, all the photons in the reconstructed *ring*

$$\chi^2_{mass} = \sum_{k=1}^{N^{photon}} \frac{(\theta^{photon}_{rec,\ k} - \theta^{ring}_{mass})^2}{(\sigma^{photon}_{\theta})^2}$$

The value of the χ^2_{mass}, (or the corresponding probability) is then used to choose among the different mass hypotheses.
σ^{photon}_{θ} is the standard deviation of the distribution of θ^{photon}_{rec}, the angle each photon reconstructed in the *ring* makes with the particle trajectory, and it is assumed to be a function of the particle β. σ^{photon}_{θ} is also used in the reconstruction to define the number of photons belonging to the *ring* (i.e. χ^2_{mass}) requiring typically $\mid \theta^{photon}_{rec} - \theta^{ring}_{rec} \mid \leq 3\sigma^{photon}_{\theta}$, where θ^{ring}_{rec} is the reconstructed Cherenkov emission angle.

σ^{photon}_{θ} has been evaluated independently using large (6 σ) cuts in the *ring* reconstruction definition. Refer to fig. 19 of report [1] for the distribution of $\theta^{photon}_{rec} - \theta^{ring}_{rec}$ in bins of β; in each bin the distribution has been fitted with a gaussian plus a linear

background to extract the resolution in θ^{photon}_{rec}.
Fig.1 shows the fit to $\sigma^{photon}_{\theta}(\beta) = a + b(1-\beta^2)$, with a = 0.8 and b = 62., which has been used in the analysis; the dependence on β results rather small, as expected.

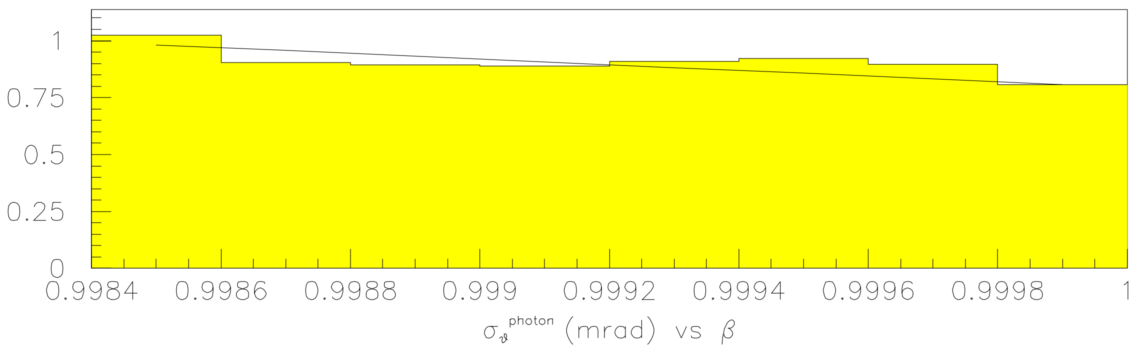

Figure 1: σ^{photon}_{θ} as a function of β from report [1]; the fit is to the form $a + b(1-\beta^2)$, with a = 0.8 and b = 62.; the result in almost a constant.

As discussed in [1] and as expected, the RICH is not able to separate $\mu's$ from higher masses and an independent μ identification is necessary.
We will take into account in the analysis only the π, K or p mass hypotheses.

b) Improved χ^2.

To try to improve the χ^2 we introduce a σ^{photon}_{θ} function of the photon azimuthal angle around the particle direction.
Let us remind that the reconstruction procedure is carried out in the plane θ^{photon}, ϕ^{photon}, the polar and the azimuthal angles of the photon around the particle trajectory.
It is known from previous studies (see [2] [3]) that the reconstructed θ^{photon} distribution varies in width as a function of ϕ^{photon}. Spherical aberrations and the use of an average photon emission point on the particle trajectory inside the radiator are responsible for this dispersion. Note that in the θ^{photon}, ϕ^{photon} plane the average photon position is on a circle of fixed radius (θ^{ring}); on the detector plane this figure is further complicated by the the fact that the detector surface is planar and at a fixed angle for all particle trajectories, resulting in an approximate elliptical shape.

To study the dependence of σ^{photon}_{θ} on ϕ^{photon} we define ϕ^{photon}_{P} with respect to the 'particle-plane', the symmetry plane which contains the particle trajectory and the mirror centre. In this way the ϕ^{photon}_{P} definition is consistent for photons of different particles.

$$\cos\phi^{photon}_{P} = \frac{(\hat{\nu}\times\hat{P})\cdot(\hat{P}\times\hat{R})}{\sin\theta^{photon}\sin\alpha}$$

where $\hat{\nu}$ is the photon direction, $\hat{P}$ the particle direction and $\hat{R}$ the mirror-centre to particle-impact-on-mirror unit vector in the Mirror Working Reference (MWR : origin in the mirror centre, z-axis normal to the detector surface); α is the angle between $\hat{P}$ and $\hat{R}$.

In fig.2 is shown the plot of θ^{photon}_{rec} - θ^{ring}_{rec} as a function of ϕ^{photon}_{P}; the variation of the width of the distribution is appreciable.

Slices of the plot along θ_{rec}^{photon} - θ_{rec}^{ring}, 15 degrees wide (see an example in fig.3), are fitted with a gaussian distribution; the resulting standard deviation (σ_{θ}^{photon}) is plotted (see fig.4) versus ϕ_{P}^{photon}.
A fit is then performed to a form

$$\sigma_{\theta}^{photon}(\phi) = a + b\cos\phi + c\cos 2\phi + d\cos 3\phi + e\cos 4\phi$$

with a = 0.775, b = 0.015, c = -0.059, d = 0.071 and e = 0.058.

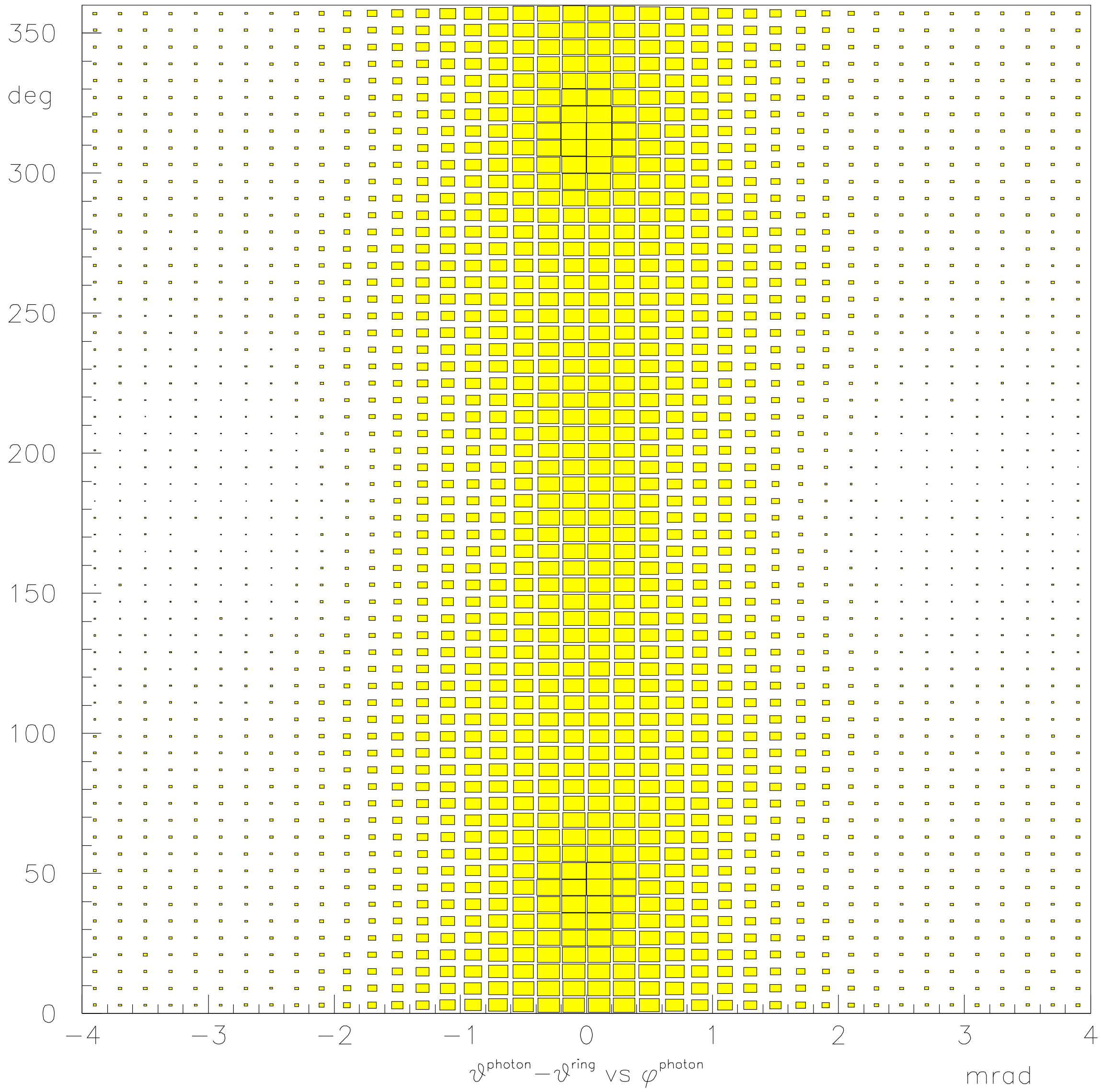

Figure 2: The distribution of θ_{rec}^{photon} - θ_{rec}^{ring} as a function of ϕ_{P}^{photon} See the text for the definition of ϕ_{P}^{photon}.

The χ^2_{mass} is then modified as

$$\chi^2_{mass} = \sum_{k=1}^{N^{photon}} \frac{(\theta_{rec,\ k}^{photon} - \theta_{mass}^{ring})^2}{(\sigma_{\theta,\ k}^{photon})^2}$$

where $\sigma_{\theta,\ k}^{photon} = \sigma_{\theta}^{photon}(\phi_{P,\ k}^{photon})$

In fig.5 the distribution of the least χ^2_{mass} normalized to N^{photon}, is shown; the broken line is the expected average value, to be compared with the actual value, in the upper

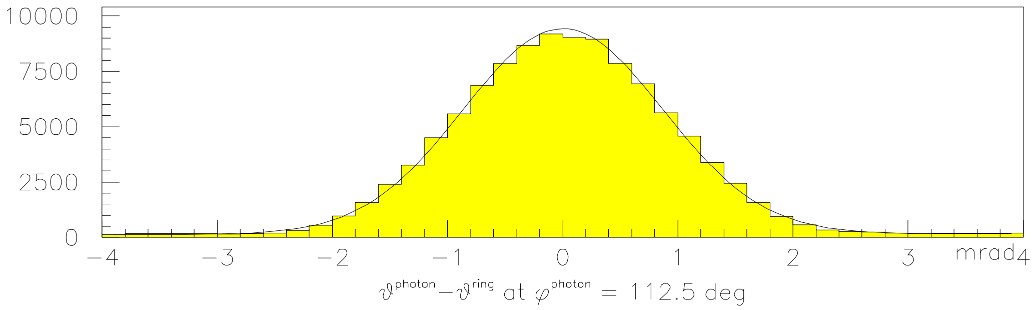

Figure 3: Example of the distribution of θ_{rec}^{photon} - θ_{rec}^{ring} for fixed ϕ_P^{photon} (112.5 ± 7.5 deg); the fit is to a gaussian plus a linear background. See the text for the definition of ϕ_P^{photon}.

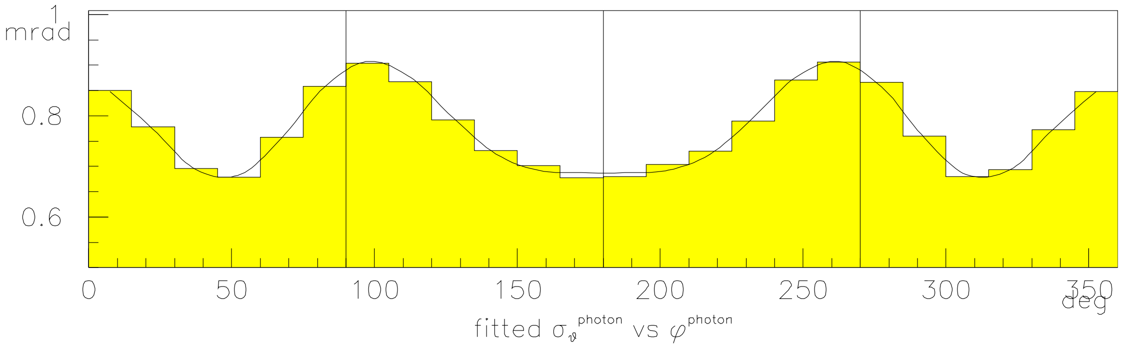

Figure 4: σ_θ^{photon} as a function of ϕ_P^{photon}; the fit is to the form $a + b\cos\phi + c\cos 2\phi + d\cos 3\phi + e\cos 4\phi$.

right corner, larger than 1 mainly because of the tail of the distribution.

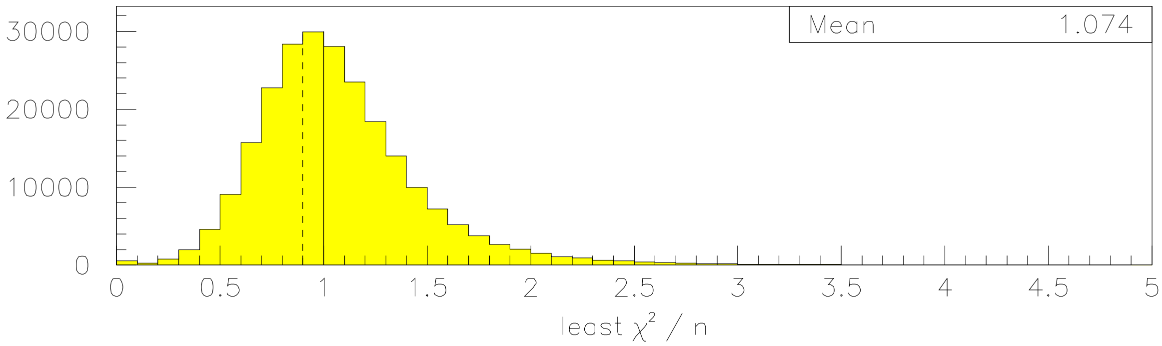

Figure 5: The distribution of the least (improved) χ^2_{mass}, normalized to the number of photons per *ring*, among the different mass hypotheses.

In table 1 the particle mass assignments are reported according to the procedure described above (improved χ^2_{mass}); the columns represent the particle types known from MC input; the rows, the particle types as identified.

Note that table 1 and the corresponding table of report [1] are not immediately comparable for two reasons :
– first, in the table of fig.21 of report [1] are not entered the mass assignments in which the χ^2_{mass} probability is zero (within the computational accuracy), as not significant. This is correct, but we have to take into account the corresponding loss of efficiency in the

PID procedure because for these particles there is no mass assignment. In table 1 all mass assignments are entered.
For a more significant mass assignment, the sample should be cleaned in some way. One can simply ask the largest probability to be greater than a fixed quantity or put some limits on the ratio between the largest probability and the second largest probability.
Studying the wrong mass assignments, one learns that many of them ($\simeq 50\%$) correspond to $K's$ and $p's$ close to the Cherenkov threshold and then with a small number of photons in the *ring*, which is at the origin of the confusion; a cut on this number seems a more natural way to get more significant mass assignments. In fig.6 is shown the momentum (a) and the number of photons N in the *ring* distribution (b) for $K's$ identified as $\pi's$; in (c) and (d), $p's$ identified as $\pi's$ or $K's$; the vertical bars in (a) and (c) are the momentum threshold. From (b) or (d) we can estimate the effects of a cut in (N) to reduce the wrong mass assignments (e.g., broken line, reject *rings* with 6 or less photons).
– second, in table 1 are not entered particles (as known from MC generation) under Cherenkov threshold; for comparison, in the table of fig.22 of report [1], in the first momentum bin, ranging from 0. to 5. GeV/c (in fact from 1.9, the μ threshold, to 5.), should not enter any Cherenkov emitting K (threshold at 8.9 GeV/c); the $K's$ identified as $\pi's$ are interacting or decaying $K's$ which give origin to a radiating particle; the same happens in the second bin up to the threshold and for protons too (threshold at 17. GeV/c). For momenta above 10 Gev/c, $K's$ wrongly identified reduce to $\simeq 0.3\%$.
This is a physical effect which should be kept separated from the RICH identification power; nevertheless on data this will be a further source of misidentification.

Quantitatively, from table 1, one can say that $\sim 1.\%$ of the $K's$ are identified as $\pi's$ or $p's$; moreover $\sim 0.9\%$ of the particles identified as $K's$ are not.
Let also note that the contents of the table of fig.21 of report [1] (not shown), when filled in the same way as table 1, as discussed above, exhibit no appreciable difference with those of table 1 itself; i.e., there is no real improvement going from the first approach to the improved χ^2 one.

	π	K	p
p	8	2	1152
K	32	6280	32
π	139811	106	21

particle identification table

Table 1: Particle mass assignments using the improved χ^2_{mass} for π, K and p; the columns represent the particle types known from MC input; the rows, the particle types as identified.

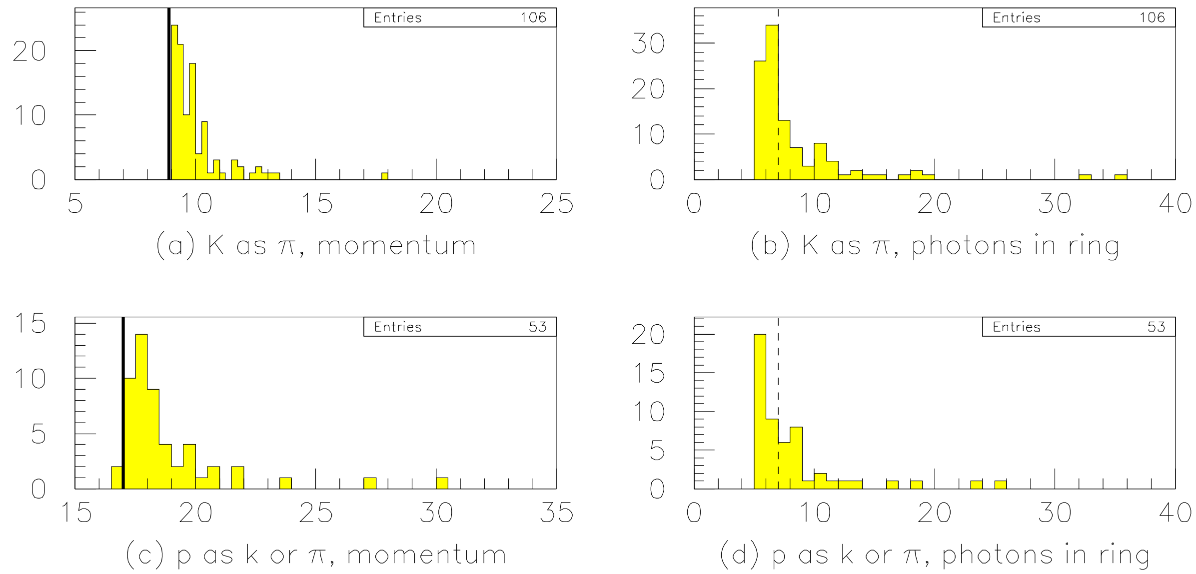

Figure 6: The figure shows (a) the momentum distribution and (b) the number of photons N in the $ring$ for $K's$ identified as $\pi's$; in (c) and (d) the same for $p's$ identified as $\pi's$ or $K's$; the vertical bars in (a) and (c) are the momentum thresholds for Cherenkov emission.

Table 2 shows the same results as in table 1, in momentum bins of 5.GeV/c, from 0. to 60.GeV/c.

3 PARTICLE IDENTIFICATION ON LIKELIHOOD BASIS

In a Likelihood estimation both the signal and the background should be described correctly.
If, as in the our case, the theoretical description is not easy, the distributions can be taken from the experimental data (MC data in this study). As shown in fig.3, in the θ^{photon}, ϕ^{photon} plane, the signal can be described quite reasonably by a gaussian distribution around θ^{ring}_{rec} with a standard deviation $\sigma^{photon}_{\theta}(\phi^{photon}_{P})$.
The background due to the electronic noise of the detector (uniformly distributed on the detector surface) can be described by a function like $B(\theta, \phi) \sim \theta$; for other sources of background, like the photons emitted by the other particles of the same event or recorded because of the memory time of the photon chambers, the description is less evident. At present we assume this background again as uniformly distributed on the detector surface and we determine its amount from data.

We can write the probability density of the photons in a $ring$ as

$$L = \prod_{k=1}^{N^{photon}} (1-\epsilon)\, \frac{1}{\sigma^{photon}_{\theta,\ k}\sqrt{2\pi}}\, \frac{(\theta^{photon}_{rec,\ k} - \theta^{ring}_{mass})^2}{2(\sigma^{photon}_{\theta,\ k})^2} + \epsilon\, \frac{2\,\theta^{photon}_{rec,\ k}}{(\theta_{Max})^2}$$

where $\sigma^{photon}_{\theta,\ k} = \sigma^{photon}_{\theta}(\phi^{photon}_{P,\ k})$ and θ_{Max} is the upper limit of θ^{ring}_{rec} range.

The background fraction ϵ is defined as $\epsilon = \frac{N_B}{(N_S+N_B)}$, where N_S is the number of photons in the gaussian peak ($ring$) and N_B is the number of photons in the background in the θ^{photon}_{rec} range from 0. to θ_{Max}.

	π	K	p
p			
K			
π	49308		

PID, mom = 2.5

	π	K	p
p			
K	1	289	
π	49350	73	

PID, mom = 7.5

	π	K	p
p			
K	13	2629	
π	20000	29	

PID, mom = 12.5

	π	K	p
p	1		238
K	6	1524	28
π	9858	1	17

PID, mom = 17.5

	π	K	p
p	3		430
K		826	3
π	5346		3

PID, mom = 22.5

	π	K	p
p			228
K	1	458	1
π	2969		

PID, mom = 27.5

	π	K	p
p	3		132
K	1	256	
π	1596	1	1

PID, mom = 32.5

	π	K	p
p		1	67
K		144	
π	743	1	

PID, mom = 37.5

	π	K	p
p	1	1	33
K	7	79	
π	386		

PID, mom = 42.5

	π	K	p
p			16
K	1	41	
π	180		

PID, mom = 47.5

	π	K	p
p			6
K	2	20	
π	61	1	

PID, mom = 52.5

	π	K	p
p			2
K		14	
π	14		

PID, mom = 57.5

Table 2: Particle mass assignments for π, K and p, in momentum bins of 5.GeV/c, from 0. to 60.GeV/c.

ϵ is evaluated from the distribution of θ_{rec}^{photon}, in bins of θ_{rec}^{ring}; in fig.7 an example of the distribution of θ_{rec}^{photon} in 8 bins of θ_{rec}^{ring}, 3 mrad wide, from 27. to 51. mrad, is shown . The fits are to a gaussian shape plus a linear background through 0.
In fig.8 the distribution of ϵ, as from the fits, in 15 bins of θ_{rec}^{ring}, from 10. to 55. mrad; the linear fit is of the form $a + b\theta$, with $a = 0.78.$ and $b = 0.0079$.

The mass assignments are then done on the basis of the largest Likelihood probability among the different mass hypotheses.
In fig.9 the distribution of the largest Likelihood, normalized ($\sqrt[n^{th}]{L}$) to the number of photons in the *ring*, is shown. In table 3 the Likelihood based particle mass assignments. From the comparison with table 1, the improvement in mass separation is appreciable; with the same particles in input, the number of $K's$ indentified as $\pi's$ is about 40.% less and the same for $p's$ indentified as $K's$, noting that the number of the well indentified $K's$ or $p's$ increases accordingly. This improvement is clearly due to the fact that the

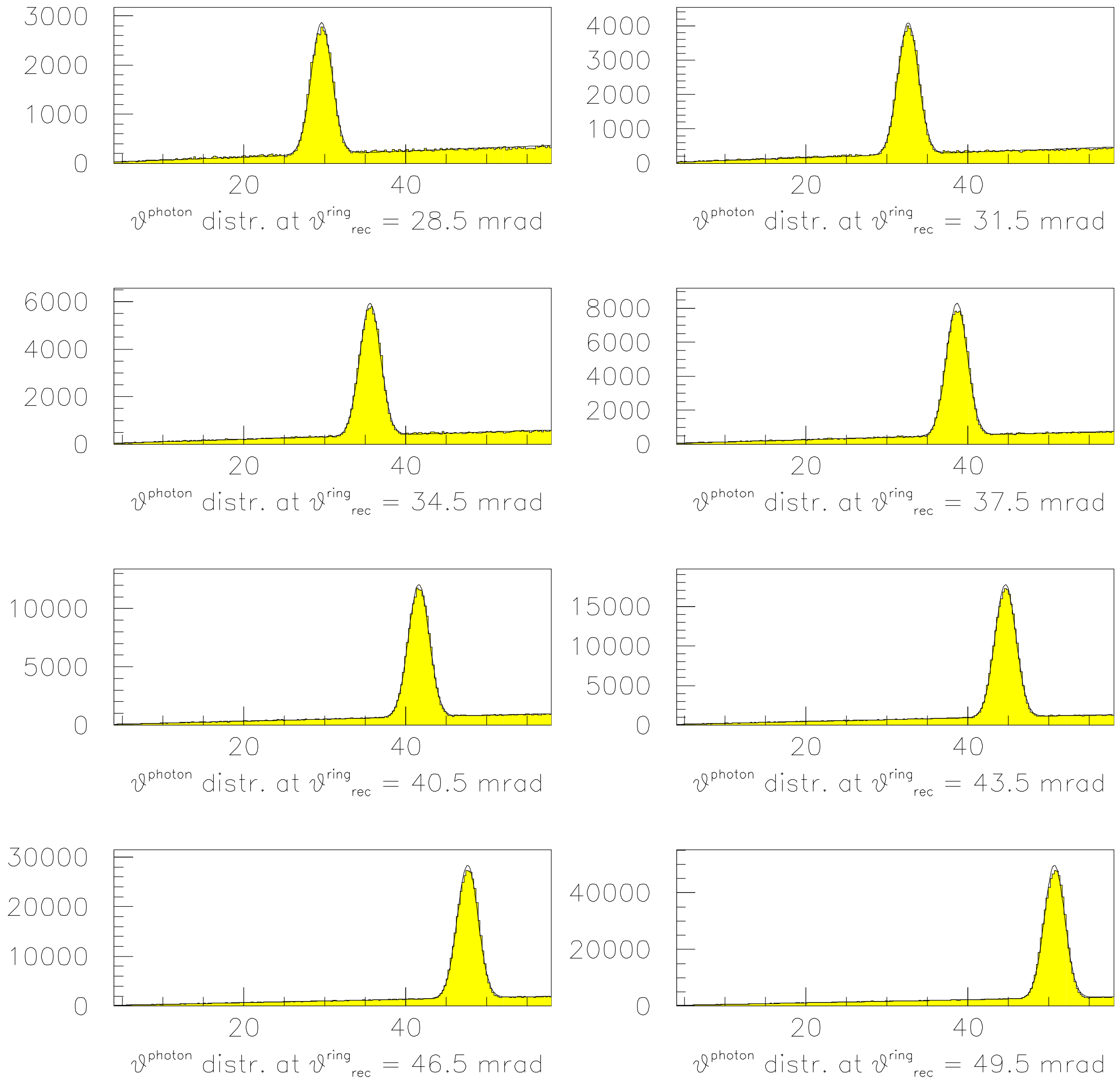

Figure 7: An example of the distribution of θ_{rec}^{photon} in 8 bins of θ_{rec}^{ring}, 3 mrad wide, from 27. to 51. mrad. The fits are to a gaussian shape plus a linear background through 0.

background is taken into account in the PID.

4 POSSIBLE IMPROVEMENTS

In principle the number of photons expected in the *ring* could be used in the definition of the Likelihood; but it is not straightforward. It depends on the particle path length inside the radiator, on the photon absorption in the gas, which are not taken into account at present, and more.

The fraction of photons lost because of the dead zones in the mirror wall or in the photon chambers, can be evaluated from the data; the photons reflected part from the upper and part from the lower mirror surface are treated together and give no problem. On the contrary, photons lost because out of the mirror or detector surface limits (and do not forget the beam pipe too) will cause some problem to this approach.

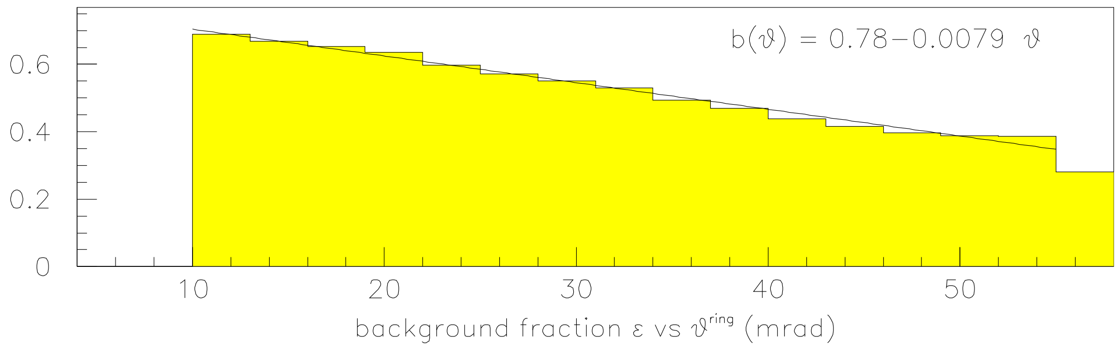

Figure 8: The figure shows the distribution of the background fraction ϵ as a function of θ_{rec}^{photon}; the line is a fit to the linear form indicated.

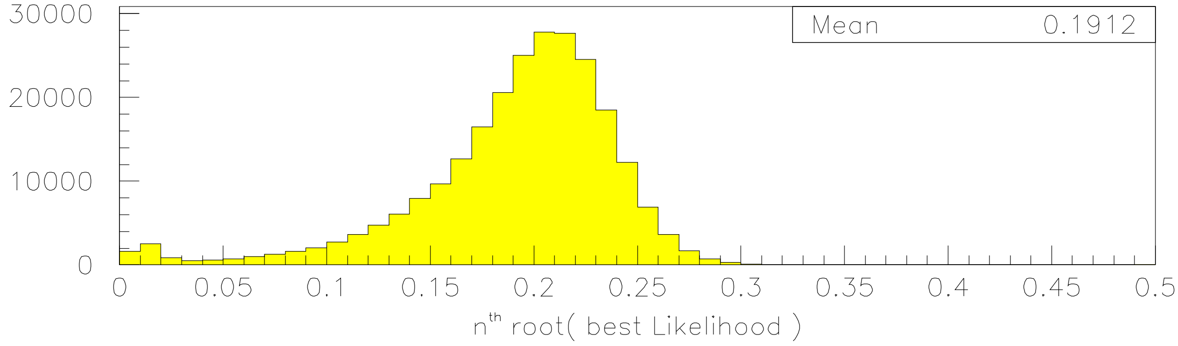

Figure 9: The distribution of the best Likelihood, normalized ($\sqrt[n^{th}]{L}$) to the number of photons.

Looking at fig.10, the spread of the difference between the reconstructed and the expected (plus background) number of photons per *ring* seems too large, in the present understanding, to allow such an approach, but further studies are on the way.

5 CONCLUSIONS

Building a Likelihood function of the photons in the *ring*, some improvement has been obtained in the RICH mass identification power. The results are promising and further studies are certainly needed.

References

[1] P. Schiavon, "Trieste reconstruction software for COMPASS RICH 1", December 1999; on COMPASS Web

[2] P. Schiavon, "Studies of the Cherenkov emission angle reconstruction", Part 1, June 1997; on COMPASS Web

[3] P. Schiavon, "Studies of the Cherenkov emission angle reconstruction", Part 2, October 1997; on COMPASS Web

	π	K	p
p	7	2	1163
K	35	6323	20
π	139809	63	22

particle identification table

Table 3: Particle mass assignments using the Likelihood approach for π, K and p; the meaning is the same as in table 1.

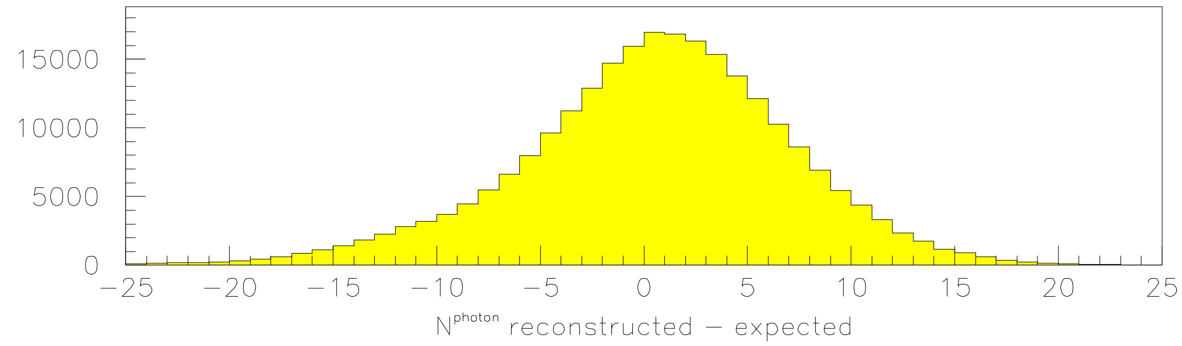

Figure 10: The distribution of the difference between the reconstructed and the expected (plus background) number of photons per *ring*; the spread is quite large.